ISSN Online: 2756-3898, ISSN Print: 2714-500X https://doi.org/10.47514/phyaccess.2022.2.1.001

Optimization of Absorber and ETM Layer Thickness for Enhanced Tin based Perovskite Solar Cell Performance using SCAPS-1D Software

Eli Danladi[1], Abdulazeez O Salawu[2], Muhammed O Abdulmalik[3], Emmanuel D Onoja[1], Elijah E Onwoke[1] and Damilare S Adepehin[1]

[1] Department of Physics, Federal University of Health Sciences, Otukpo, Benue State, Nigeria.
[2] Department of Computer Science, Nile University of Nigeria., Nigeria.
[3] Department of Physics, Confluence University of Science and Technology, Osara, Kogi State, Nigeria.

Corresponding E-mail: danladielibako@gmail.com

Received 04-02-2022
Accepted for publication 28-02-2022
Published 04-03-2022

Abstract

The methyl ammonium tin iodide ($CH_3NH_3SnI_3$) perovskite nanocrystals have attracted research interest and have become a rising star in the horizon of photovoltaics due to its narrow band gap, wide visible absorption coefficient and environmental friendliness than its lead-based counterpart ($CH_3NH_3PbI_3$). In this article, a tin based perovskite solar cell with Zinc oxide (ZnO) and Copper Oxide (CuO) as electron transport medium (ETM) and hole transport medium (HTM) was proposed and investigated numerically using a Solar Cell Capacitance Simulator (SCAPS) tool. With appropriate parameters, a short-circuit current density (Jsc) of $27.56\ mA/cm^2$, open-circuit voltage (Voc) of $0.82\ V$, fill factor (FF) of 59.32 %, and power conversion efficiency (PCE) of 13.41 % are obtained for the initial simulation. By varying the thicknesses of the absorber and electron transport layer, the optimum thicknesses were observed at $0.6\ \mu m$ and $0.3\ \mu m$ for $CH_3NH_3SnI_3$ and ZnO with corresponding PCEs of 14.36 % and 13.42 %. Upon simulation with optimized parameters, a Jsc of $29.71\ mA/cm^2$, Voc of $0.83\ V$, FF of 61.23 % and PCE of 15.10 % were recorded. These values are superior to those obtained without optimization which means that solar cell performance can be improved to some extent by adjusting the perovskite and electron transport layer and also, $CH_3NH_3SnI_3$ Perovskite solar cell (PSC) is a potential environmentally friendly solar cell with considerable efficiency.

Keywords: Electron transport layer; Perovskite solar cells; SCAPS; Perovskite absorber

I. Introduction

Organic–inorganic hybrid perovskite nanocrystals have shown the most promising candidacy for high efficient and low-cost solar cells. Halide perovskites have the formula of ABX_3 [1], where A is the cation including MA^+, FA^+, Cs^+, etc., B is Pb^{2+} or Sn^{2+}, and the anion X is a halogen ion (usually I^-, Br^-, or Cl^-). Ideally, it has a cubic crystal structure consisting of a corner-sharing BX6 octahedral network with a cation in the interstices. Halide perovskite nanocrystal has the unique property of weak exciton binding energy [2, 3] which means light induced excitons will dissociate into free carriers quickly at room temperature. Perovskite materials are characterized with a long carrier diffusion length and high carrier diffusion velocity [4-6].

Reported perovskite covers a wide range of band gap energies, from $MASnI_3$ (1.1 eV), $MAPbI_3$ (1.6 eV), $MAPbBr_3$ 2.3 eV) to $MAPbCl_3$ (3.1 eV) [7]. Furthermore, by fine tuning the composition of cations (MA^+, Cs^+, FA^+, Rb^+ etc.) and anions (Cl^-, Br^-, I^- etc.), it is also possible to vary the absorption spectrum [8]. The application of perovskite nanocrystals was first introduced into dye sensitized solar cell (DSSC) to replace dye pigment by Kojima et al. [9] which results to a record PCE of 3.80 %. Since from then, several device modification and device engineering were done to achieve a PCE > 25 % recently [10].

TiO_2 is considered the mostly used ETM for PSCs device due to its high performance in solar cells as a result of its proper band gap and high transmittance. However, obtaining good quality film of either compact or mesoporous TiO_2 requires high annealing temperature, which limits its application in solar devices and results to increase in the production cost. Consequently, the electron mobility of perovskite materials is $\sim 7.5\ cm^2V^{-1}s^{-1}$ and that of TiO_2 ranged between 0.1– 4.0 $cm^2V^{-1}s^{-1}$. These lower values of electron mobility in TiO_2 may result to shortfall in performance of solar cells [11].

Other alternatives to TiO_2 include SnO_2 [12-13], ZnO [14-15], SiO_2 [16-17], Al_2O_3 [18-19] and ZrO_2 [20]. For SiO_2, Al_2O_3 and ZrO_2, the band gap is larger, and the conduction band edge is much higher than the conduction band of the perovskite layer which prevents smooth electron injection into both SiO_2, Al_2O_3 and ZrO_2. Thus, the excited electron remains in the conduction band of the perovskite layer for a longer time [21]. Among them, zinc oxide has many properties that can be used in PSCs, such as high transmittance in the visible spectra and more importantly, its low cost and much higher electron mobility of $115 - 155\ cm^2V^{-1}s^{-1}$ which can potentially improve the electron transport efficiency and reduce the recombination loss as an ETM [4, 22-24].

The ETM is used to compensate and balance the difference of hole and electron diffusion lengths [2, 4]. In addition, the ETM is a blocking layer that prevents holes from reaching the fluorine-doped tin oxide (FTO) electrode. For high performance solar cells, ETMs should meet the following criteria: (a) good optical transmittance in the visible range, which reduces the optical energy loss; (b) the energy levels of ETMs should match that of perovskite materials, which improve the electron extraction efficiency and block holes; (c) good electron mobility. As a result, the design and materials properties of the ETM are crucial for solar cell performance [2-4, 25].

Lead based perovskites materials are considered as promising candidates for future-generation photovoltaics owing to their unique optoelectronic properties and very low fabrication cost. Despite its exhibited properties, the presence of toxic lead poses a severe concern regarding their environmental friendliness and practical deployment [26]. Furthermore, the intrinsic band gaps that are generally greater than 1.5 eV have prevented the realization of its predicted theoretical value. Based on the above known facts, tin halide perovskites have displayed some properties as alternative candidates to lead based absorber. Tin based have large carrier mobility and strong light absorption coefficients due to its electronic configurations similar to those of lead based. Moreover, the band gaps of tin perovskites can be tailored to ~1.4 eV, approaching the ideal band gaps for single-junction solar cells [10]. Although the overall PCE of tin base is still much lower than that of lead base at present, the field is witnessing their continued rapid progress, as compared to lead base that have actually reached attained level in their development. In this regard, tin is very promising because it combines the merits of high performance, low cost, and the absence of lead metal.

The properties for the layers (absorber and ETM) make them (ZnO a promising ETM and $CH_3NH_3SnI_3$ a promising absorber) for PSCs. Meanwhile, although most physical properties of ZnO and TiO_2 are similar, there are also some distinct properties for each material. As a result, studies on ZnO based solar cells will enrich the family of PSCs, which will in turn help to improve the performance of PSCs.

In this article, we designed and studied perovskite solar cells based on ZnO and $CH_3NH_3SnI_3$ as ETM and absorber using SCAPS-1D. The effect of varying the thickness of various layers through getting the optimized values were explored systematically. The results show that, thickness of absorber and ETM are essential factors to be considered in a solar cell.

II. MODELING AND SIMULATION

The modeling of the solar cell was done using SCAPS [27-29]. The software is based on the basic equations of the semiconductor: hole (1) and electrons (2) continuity equations together with Poisson equation (3) as follows [30]:

$$\frac{dp_n}{dt} = G_P - \frac{P_n - P_{n0}}{\tau_p} - p_n\mu_p\frac{dE}{dx} - \mu_P E\frac{dp_n}{dx} + D_P\frac{d^2p_n}{dx^2} \quad (1)$$

$$\frac{dn_p}{dt} = G_n - \frac{n_p - n_{p0}}{\tau_n} - n_p\mu_n\frac{dE}{dx} - \mu_n E\frac{dn_P}{dx} + D_n\frac{d^2n_p}{dx^2} \quad (2)$$

$$\frac{d}{dx}\left(-\varepsilon(x)\frac{d\psi}{dx}\right) = q[p(x) - n(x) + N_d^+(x) - N_a^-(x) + p_t(x) - n_t(x)] \quad (3)$$

Where $N_a^-(x)$ denotes ionized acceptor-like doping concentration and $N_d^+(x)$ denotes ionized donor-like doping concentration. $n_t(x), p_t(x), n(x), p(x)$ refer to trapped holes, free electrons and free holes respectively, x is the direction along the thickness, D is diffusion coefficient, G is generation rate, E is electric field, q is electron charge, ε permittivity and ψ is electrostatic potential. By obtaining the solution of the above equations, outputs such as the recombination profile, current voltage characteristics, spectral response and band diagram can be gotten. The device structure of the simulated PSCs is considered with layer configuration as shown in Fig. 1. All the data used in the simulation is as summarized in Tables I and II [14, 30, 31-35].

Table I Parameters used for simulation of perovskite solar cell structures using SCAPS-1D.

Parameters	TCO	ETM (ZnO)	Absorber	HTM (CuO)
Thickness (μm)	0.5	0.055	0.40	0.15
Band gap energy Eg (eV)	3.5	3.3	1.30	1.3
Electron affinity χ (eV)	4.0	4.0	4.20	4.07
Relative permittivity ϵ_r	9	9.0	8.2	18.1
Effective conduction band density Nc (cm^{-3})	2.0×10^{18}	3.7×10^{21}	1.0×10^{18}	2.8×10^{19}
Effective valance band density Nv (cm^{-3})	1.8×10^{19}	1.8×10^{19}	1.0×10^{18}	2.8×10^{19}
Electron mobility μn ($cm^2 V^{-1}s^{-1}$)	20	100	1.6	0.1
Hole mobility μp ($cm^2 V^{-1}s^{-1}$)	10	25	1.6	0.1
Donor concentration ND (cm^{-3})	2×10^{19}	1×10^{18}	0	0
Acceptor concentration NA (cm^{-3})	0	0	3.2×10^{15}	1×10^{18}
Defect density Nt (cm^{-3})	1×10^{15}	1×10^{13}	4.5×10^{16}	1×10^{15}

Table II Parameters of interface layer

Parameters	$CH_3NH_3SnI_3$	$ZnO/CH_3NH_3SnI_3$ interface	$CH_3NH_3SnI_3/CuO$ interface
Defect type	Neutral	Neutral	Neutral
Capture cross section for electrons (cm^2)	2×10^{-14}	2×10^{-15}	2×10^{-15}
Capture cross section for holes (cm^2)	2×10^{-14}	2×10^{-15}	2×10^{-15}
Energetic distribution	Gaussian	Single	Single
Energy level with respect to Ev (eV)	0.650	0.650	0.650
Characteristic energy (eV)	0.1	0.1	0.1
Total density (cm^{-3})	10^{15}–10^{19}	1×10^{18}	1×10^{18}

We selected the parameters for the initial device from existing literatures and all acknowledged in the text. The defect interfaces are $ZnO/CH_3NH_3SnI_3$ and $CH_3NH_3SnI_3/CuO$. Thermal velocities of hole and electron are selected as $10^7\ cms^{-1}$. In the simulation studies, the influence of shunt resistance and series resistance were ignored due to power loses by providing an alternate current path for the incident current generated. Front and back contact work function are $4.0\ eV$ (FTO) and $4.47\ eV$ (silver), respectively. For the simulation under illumination the standard AM 1.5 spectrum is used and the cell operating temperature is set at $300\ K$. In our study, we optimized the device configuration as follows: The parameters of FTO, ZnO and CuO are kept unchanged and the thickness of $CH_3NH_3SnI_3$ is varied to get the optimum performance parameters. The same procedure is adopted for optimizing the thickness of ZnO used in this study by keeping the parameters of FTO, $CH_3NH_3SnI_3$ and CuO unchanged.

III. RESULTS AND DISCUSSION

A. Modeled PSC, Energy level diagram and absorption coefficient

The PSC and band structure of the tin based perovskite solar cell obtained with simulated parameters are shown in Fig. 1(a) and (b). The interface conduction and valence band offset at $ZnO/CH_3NH_3SnI_3$ and $CH_3NH_3SnI_3/CuO$ interfaces are $\Delta Ec = 0.15\ eV$ & $\Delta Ev = 2.29\ eV$ and $\Delta Ec = 0.13\ eV$ & $\Delta Ev = 0.03\ eV$ (see Fig. 1(b)). The values of ΔEc and ΔEv are beneficial for carriers in the modeled PSC.

The absorption coefficient of ZnO, $CH_3NH_3SnI_3$ and CuO (SCAPS data file) is shown in Fig. 1(c) and (d), which shows the fraction of light lost due to scattering and absorption per unit distance of the penetration medium. It is seen from Fig. 1(c) that the absorption coefficient decreases with the increase in the visible wavelength range. This indicates that the fraction of light lost due to scattering and absorbance decreases. It can also be noted from Fig. 1(d) that the value of absorption coefficient decreases with the visible region. With respect to the photon energy (see Fig. 1(d)), we observed an increase in the absorption coefficient. The increase in the absorption coefficient indicates the scattering loss of light while travelling through the medium with high absorption.

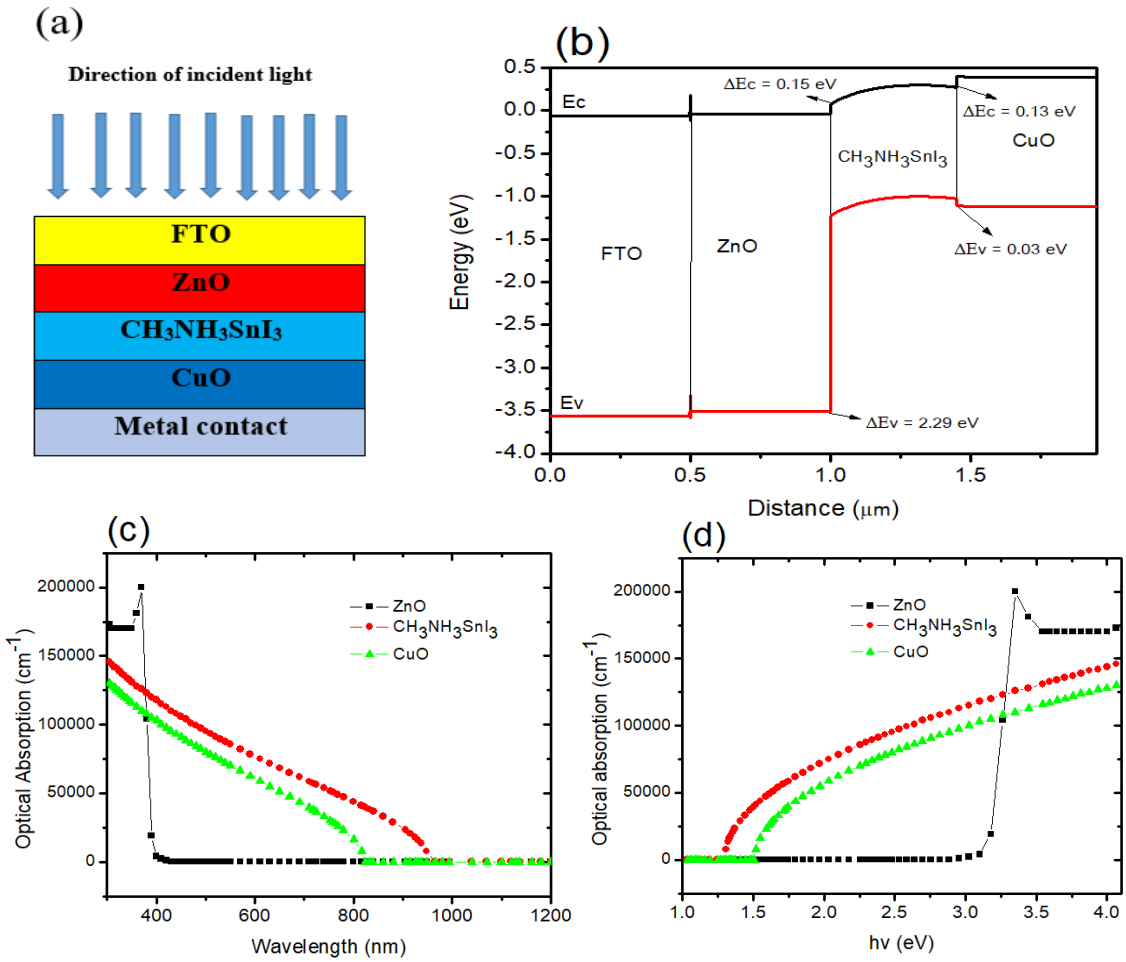

Fig. 1 (a) The structure of the simulated perovskite solar cell (b) Energy band diagram of PSC device (c) Optical Absorption vs. Wavelength of the ETM, absorber and HTM and (d) Optical Absorption vs. photon energy of the ETM, absorber and HTM

B. Analysis for initial device

With these initial parameters from Tables I and II, we studied the current density–voltage (J-V) and quantum efficiency-wavelength ($QE - \lambda$) characteristic of the cell (see Fig. 2(a) and (b)). The short-circuit current density of 27.56 mA/cm^2, open-circuit voltage of 0.82 V, fill factor of 59.32 %, and power conversion efficiency of 13.41 % are obtained. The simulated device performance is consistent with the experimental values of the Tin-based PSCs [36], certifying that the device simulation is valid and the input parameters that have been set are close to those for a real device. However, looking at the quantum measurement, the QE also increase with photon energy increase (see Fig. 2(c)). The QE covers the entire visible spectrum and reaches a broad absorption maximum $> 80\%$ from 380 nm to 980 nm (see Fig. 2(b)) which is in agreement with similar studies [32]. The sweeping at the visible and near IR region of the QE curve is beneficial to the light absorption at the various wavelengths.

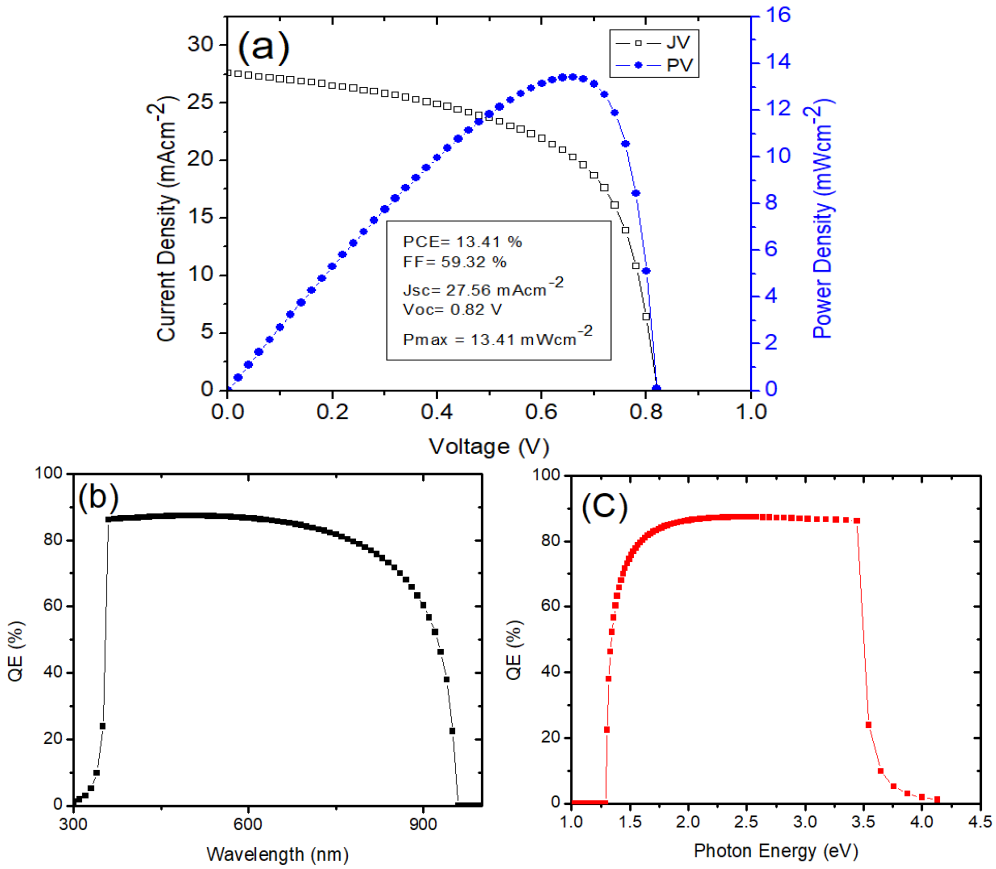

Fig. 2(a) J–V curve of PSC with initial parameters, (b) QE of the initial device with respect to wavelength and (c) QE of the initial device with respect to photon energy

C. Effect of thickness of Perovskite Absorber nanocrystal

The thickness of the light-absorbing layer plays a critical role in establishing the performance of perovskite solar cells [14, 32, 34, 37]. The variation of the cell performance with the thickness of the absorption layer is shown in Fig. 3(c-f). The thickness of absorber layer was varied from 0.1 μm to 1.0 μm. When the thickness of the absorber is too low, the absorption of light is too low and results to low PV parameters. With the increase in thickness from 0.1 μm to 0.6μm, the PCEs of the cells improve significantly and when the thickness exceeds 0.6 μm, the PCE of the cell slows down in growth, this is because, if the absorber layer is too thick (above 0.6 μm), the photogenerated carriers cannot be collected effectively because they must travel through the absorber to reach the carrier collecting layers before quenching of charge carriers take place [32].

The Voc is constant for devices with a perovskite layer thickness from 0.6 μm to 1.0 μm. The main parameter that is negatively affected by the increase of the perovskite layer thickness is the FF, which drops strongly for device thicknesses from 0.1 μm to 0.5μm. When the thickness is increased from 0.6 μm to 1.0 μm, the FF improves, as a result, the PCE also increased. This implies that the FF is related to the efficiency of charge extraction that resulted from smaller built in voltage in the thicker devices [37], which means that, increasing thickness increases the photon-capturing ability, which results in an increase in the rate of generation of charge carriers [38].

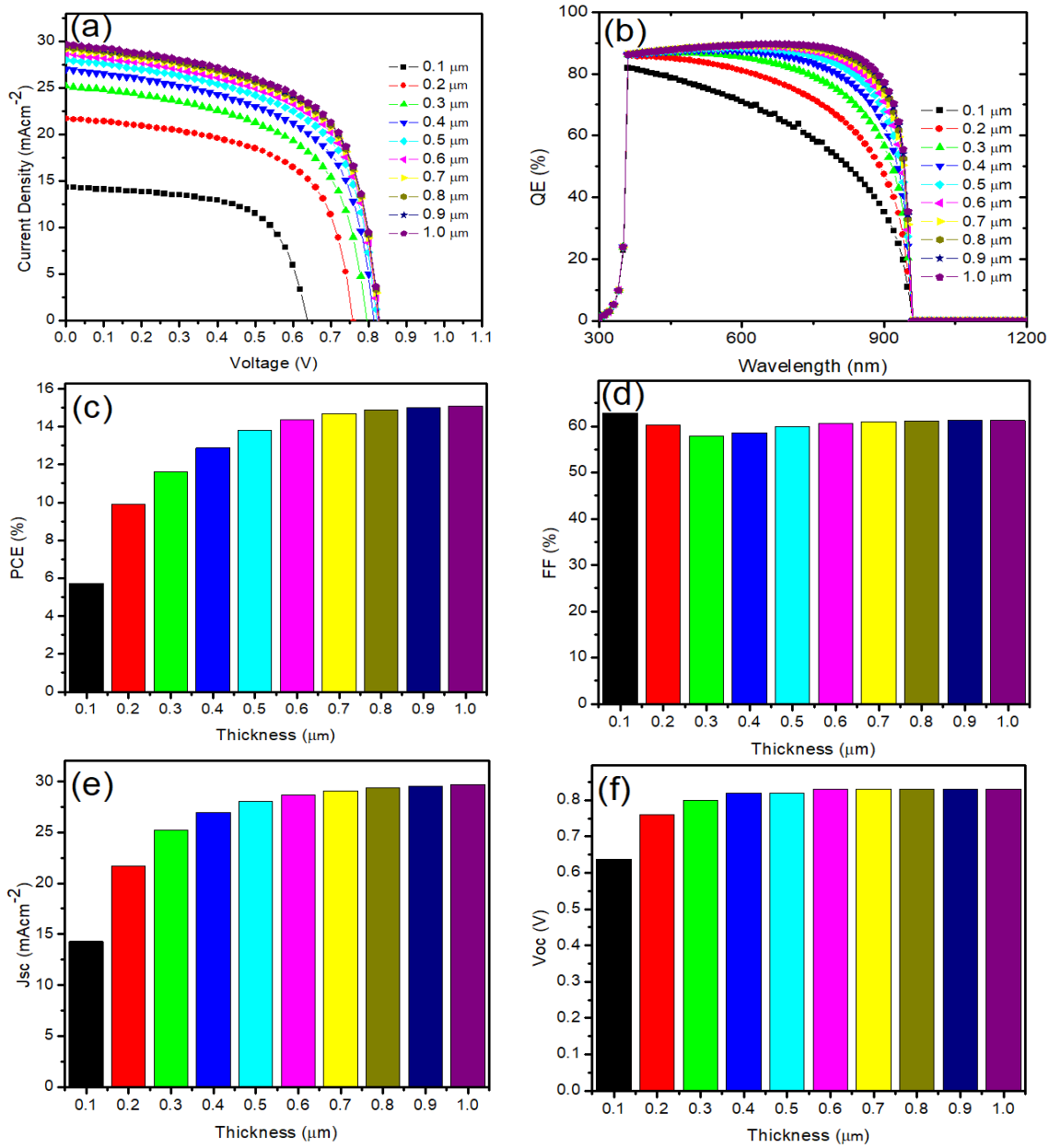

Fig. 3 (a-b) $J-V$ and $QE-\lambda$ curves of PSC with absorber thickness of 0.1, 0.2, 0.3, 0.4, 0.5, 0.6, 0.7, 0.8, 0.9 and 1.0 μm (c-f) Variation in performance parameters (PCE, FF, Jsc and Voc) of PSC with thickness of absorber.

D. Effect of thickness of the ETM

The Thickness of the ETM significantly affect the performance of a solar cell. Importantly, the selection of the appropriate ETM plays a significant role on the design and implementation of high efficiency perovskite solar cell as the energy band alignment between absorber and ETM layer is a crucial factor for the efficiency improvement of PSCs [12, 39, 40]. The variation of performance parameters with thicknesses of the ETM is shown in Fig. 4(a-d).

From the results of our simulation, the efficiency decreases slightly from 13.42 % to 13.39 % as thickness is increased from 0.3 to 1.9 μm. The results here show that, the ETM does

not have much effect on the photovoltaic parameters of the simulated perovskite solar cells. To show the less effectiveness of ETM in perovskite solar cells, some researchers have demonstrated by means of simulation and experiment that ETM-free PSCs are possible [41,42]. This can be witnessed on the basis of the fact that perovskite material itself could help the generation of charge carriers by photon excitation and ETM layer is just a charge transport layer.

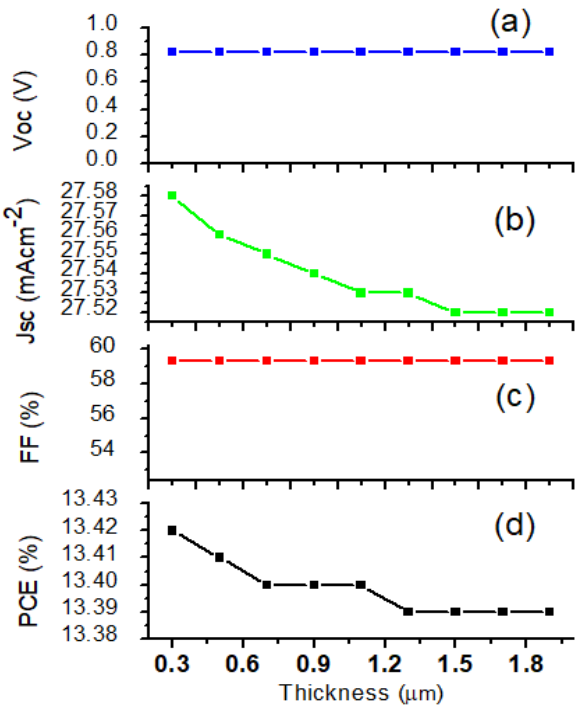

Fig. 4 Variation in performance parameters (a) Voc with thickness, (b) Jsc with thickness, (c) FF with thickness and (d) PCE with thickness of absorber.

Even in the absence of the ETM, the FTO which is an n-type layer will directly have contact with the perovskite layer and then transport the electron without affecting the PCE. Increasing the ETM layer thickness reduces the Jsc of the PSCs by increasing photon absorption and resistance of the cell (see Fig. 5 that shows increase in photon energy with increase QE which is a function of material absorption). The increased QE with increase photon energies can be attributed to the increase in absorption coefficient within the regions and consequence of increased density of localized states in the gap itself due to the rise in new defect states [43]. The optimized ETM layer thickness is 0.3 which shows PCE, FF, Jsc and Voc Values of 13.42 %, 59.32 %, 27.58 mAmcm-2 and 0.82 V.

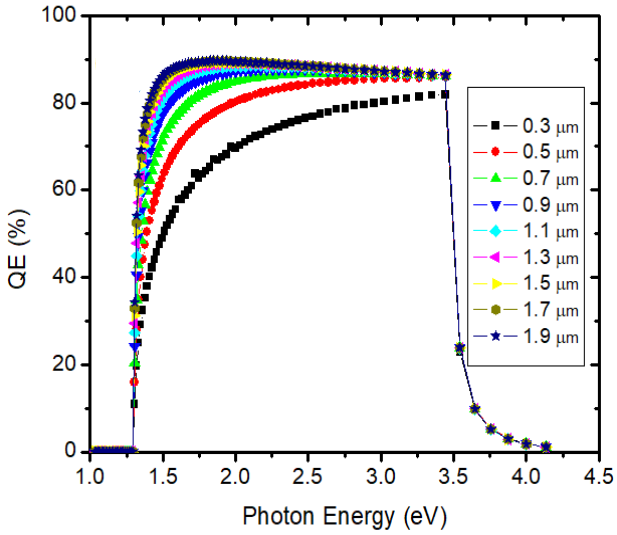

Fig. 5 QE with different values of thickness of ETM vs. wavelength

As shown, the Jsc decreases with increasing ETM layer thickness. It decreases slowly with the ETM thickness from 0.3 to 1.1 μm and it continues to maintain constant values of 27.52 $mAcm^{-2}$ at thickness of 1.3 to 1.9 μm (see Table III). The FF and Voc are constant for all devices with thickness from 0.3 to 1.9 μm (see Table III). As a result of the decreasing Jsc, the PCE also decreases with increasing ETM thicknesses at same values recorded for the Jsc which means at those thicknesses, there are no losses or gains which makes the parameters unchanged. At this point, the numbers of photo-generated carriers are equal to the number of absorbed photons. Fig. 6(a-i) describes graphically the solar cell current densities as a function of open circuit voltage.

Table III J-V characteristic parameters with the variation of thickness of ETM

Thickness (μm)	Jsc ($mAcm^{-2}$)	Jmp ($mAcm^{-2}$)	Voc (V)	Vmp (V)	FF (%)	PCE (%)
0.3	27.58	20.34	0.82	0.66	59.32	13.42
0.5	27.56	20.32	0.82	0.66	59.32	13.41
0.7	27.55	20.31	0.82	0.66	59.32	13.40
0.9	27.54	20.30	0.82	0.66	59.32	13.40
1.1	27.53	20.30	0.82	0.66	59.32	13.40
1.3	27.52	20.29	0.82	0.66	59.32	13.39
1.5	27.52	20.29	0.82	0.66	59.32	13.39
1.7	27.52	20.29	0.82	0.66	59.32	13.39
1.9	27.52	20.29	0.82	0.66	59.32	13.39

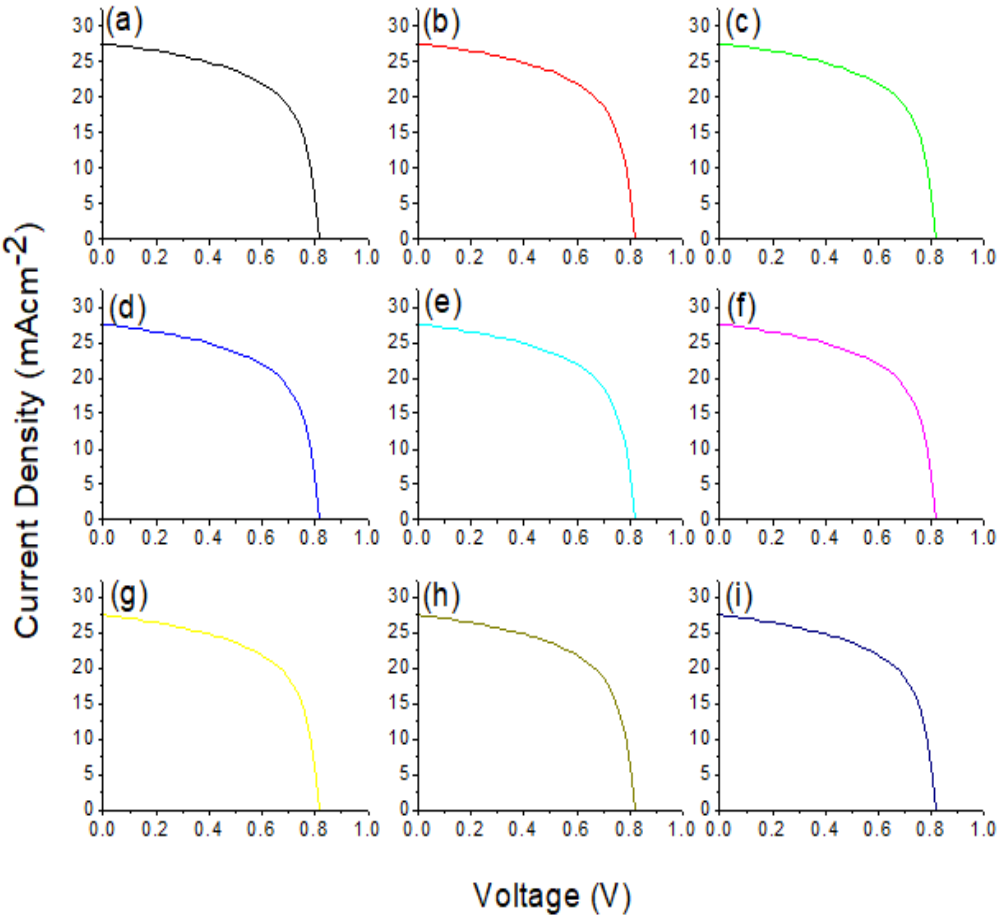

Fig. 6 J–V curves of PSC with ETM thickness of (a) 0.3 μm (b) 0.5 μm (c) 0.7 μm (d) 0.9 μm (e) 1.1 μm (f) 1.3 μm (g) 1.5 μm (h) 1.7 μm (i) 1.9 μm

E. Optimized simulated PSC, QE and Energy level diagram

Optimizing the parameters of the absorber thickness (0.6 μm) and thickness of ETM (0.3 μm), we obtained encouraging results of the Jsc of $29.71\ mAcm^{-2}$, Voc of $0.83\ V$, FF of 61.23 % and PCE of 15.10 % (see Fig. 7(a)). When the optimized results are compared with the initial device without optimization, an enhancement of ~1.13 times in PCE, ~1.08 times in Jsc, ~1.01 times in Voc and ~1.03 times in FF. From the simulated parameters, the QE vs. (wavelength and photon energy) and the energy level diagram for the optimized perovskite solar cell are shown in Fig. 7(b), (c) and (d) respectively. The conduction and valence band offset at $ZnO/CH_3NH_3SnI_3$ and $CH_3NH_3SnI_3/CuO$ interface were reduced, which can be considered beneficial for the flow of photo-excited charge carriers to prevent losses. The quantum efficiency also shows stronger absorber in the visible region and near IR region.

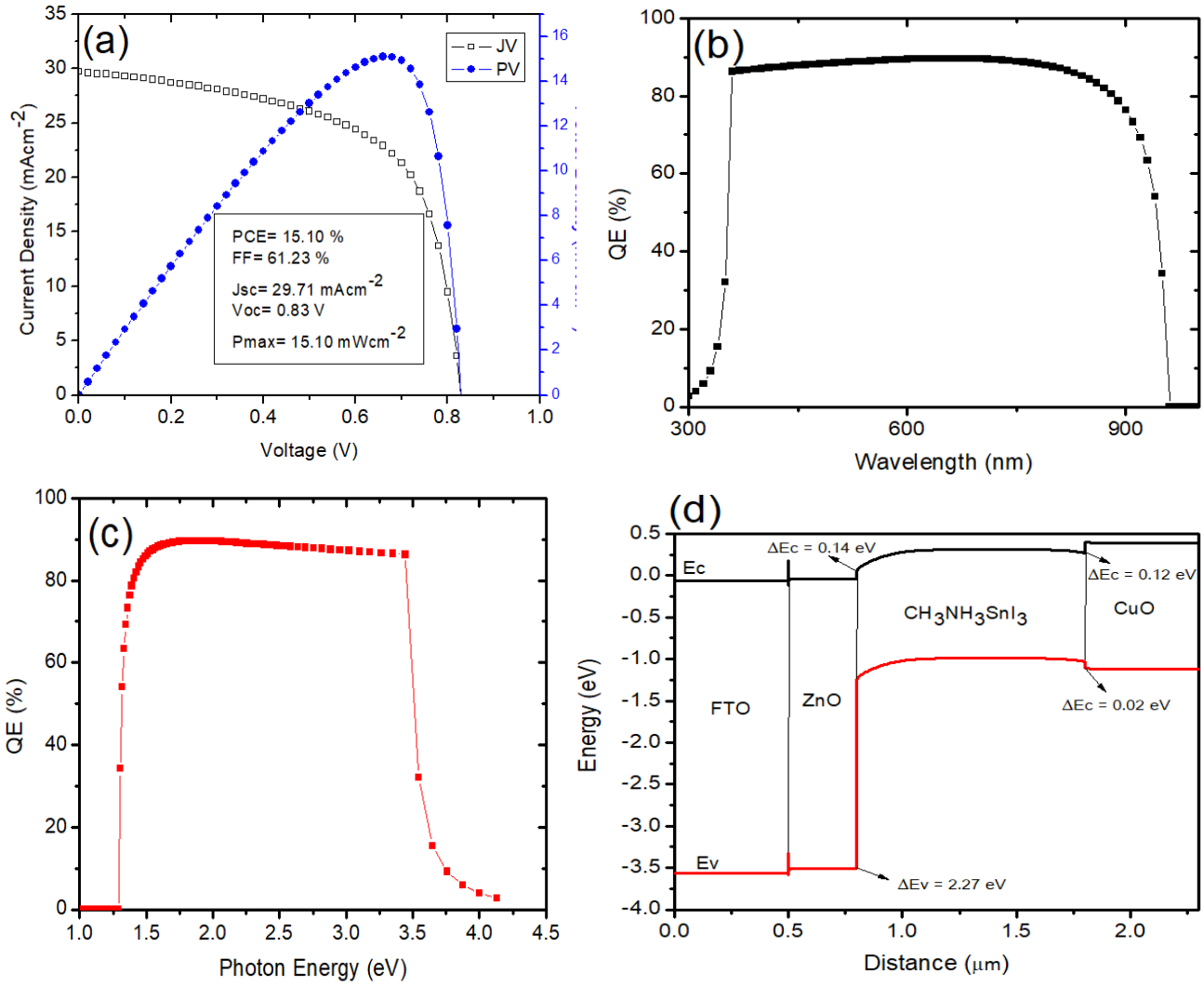

Fig. 7(a) J–V curve of PSC with optimized parameters, (b) QE of the initial device with respect to wavelength (c) QE of the initial device with respect to photon energy and (d) Energy band diagram of the optimized PSC device.

IV. Conclusion

In this paper, a numerical simulation of perovskite solar cells with configuration of $FTO/ZnO/CH_3NH_3SnI_3/CuO$ was studied using SCAPS-1D tool. Two most important factors (which are absorber and ETM thicknesses) that affect the performance of PSC were investigated. We found that these two factors influence the metrics parameters of the simulated PSCs. The results show that the optimal $CH_3NH_3SnI_3$ thickness was 0.6 μm and the optimal ZnO thickness was 0.3 μm which results to overall PSC with the following photovoltaic performance, Jsc of $29.71\ mAcm^{-2}$, Voc of 0.83 V, FF of 61.23 % and PCE of 15.10 %.

Acknowledgment

The authors would like to thank Professor Marc Burgelman, Department of Electronics and Information Systems, University of Gent for the development of the SCAPS software package and allowing its use.

References

[1] K. D. Jayan, V. Sebastian, "Comprehensive device modelling and performance analysis of MASnI3 based perovskite solar cells with diverse ETM, HTM and back metal contacts", Solar Energy, vol. 217, pp. 40-48. 2021.

[2] M. Gratzel, "The light and shade of perovskite solar cells", Nature Materials, vol. 13, pp. 838-842. 2014.
[3] G. Li, R. Zhu, Y. Yang, "Polymer solar cells", Nature Photonics, vol. 6, pp. 153-161. 2012.
[4] P. Zhang, J. Wu, T. Zhang, Y. Wang, D. Liu, H. Chen, L. Ji, C. Liu, W. Ahmad, Z. D. Chen, S. Li, "Perovskite Solar Cells with ZnO Electron-Transporting Materials", Advanced Materials, vol. 30, no. 3, 1703737. 2018.
[5] D. H. Kim, J. Park, Z. Li, M. Yang, J. S. Park, I. J. Park, J. Y. Kim, J. J. Berry, G. Rumbles, K. Zhu, "300% Enhancement of Carrier Mobility in Uniaxial-Oriented Perovskite Films Formed by Topotactic-Oriented Attachment", Advanced Materials, vol. 29, no. 3, 1606831. 2017.
[6] M. N. Hoque, N. Islam, Z. Li, G. Ren, K. Zhu, Z. Fan, "Ionic and Optical Properties of Methylammonium Lead Iodide Perovskite across the Tetragonal–Cubic Structural Phase Transition", Chemistry-Sustainability-energy-materials, vol. 9, no. 18, pp 2692-2698. 2016.
[7] Y. Hou, "Rational Interfaces Design of Efficient Organic–inorganic Hybrid Perovskite Solar Cells", Ph.D thesis, Der Technischen Fakultätder Friedrich-Alexander-UniversitätErlangen-Nürnberg, 2017.
[8] J. Berry, T. Buonassisi, D. A. Egger, G. Hodes, L. Kronik, Y. L Loo, I. Lubomirsky, S. R. Marder, Y. Mastai, J. S. Miller, D. B. Mitzi, Y. Paz, A. M. Rappe, I. Riess, B. Rybtchinski, O. Stafsudd, V. Stevanovic, M. F. Toney, D. Zitoun, A. Kahn, D. Ginley, D. Cahen, "Hybrid organic-inorganic perovskites (HOIPs): Opportunities and Challenges", Advanced Materials, vol. 27, no. 35, pp. 5102-5112. 2015.
[9] A. Kojima, K. Teshima, Y. Shirai, T Miyasaka, "Hybrid organic-inorganic perovskites (HOIPs): Opportunities and Challenges", Journal of the American Chemical Society, vol. 131, no. 7. pp. 6050-6051. 2009.
[10] X. Jiang, Z. Zang, Y. Zhou, H. Li, Q. Wei, Z. Ning, "Tin Halide Perovskite Solar Cells: An Emerging Thin-Film Photovoltaic Technology", Accounts in Materials Research, vol. 2, no. 4. pp. 210–219. 2021.
[11] H. S. Jung, N. G. Park, "Perovskite Solar Cells: From Materials to Devices", Small, vol. 11 no. 1, pp. 10-25. 2015.
[12] N. A. Sultana, M. O. Islam, M. Hossain, Z. H. Mahmood, "Comparative Performance Study of Perovskite Solar Cell for Different Electron Transport Materials", Dhaka University Journal of Science, vol. 66, no. 2, pp. 109-114. 2018.
[13] Q. Jiang, L. Zhang, H. Wang, X. Yang, J. Meng, H. Liu, Z. Yin, J. Wu, X. Zhang, J. You, "Enhanced electron extraction using SnO2 for high-efficiency planar-structure HC(NH2)2PbI3-based perovskite solar cells", Nature Energy, vol. 2, 16177. 2016.
[14] T. Ouslimane, L. Et-taya, L. Elmaimouni, A. Benami, "Impact of absorber layer thickness, defect density, and operating temperature on the performance of MAPbI3 solar cells based on ZnO electron transporting material", Heliyon, vol. 7, no. 3, e06379. 2021.
[15] F. Anwar, R. Mahbub, S. S. Satter, S. M. Ullah, "Effect of Different HTM Layers and Electrical Parameters on ZnO Nanorod-Based Lead-Free Perovskite Solar Cell for High-Efficiency Performance", International Journal of Photoenergy, vol. 9, 9846310. 2017.
[16] C. C. Tsenga, L. C. Chend, L. B. Changa, G. M. Wua, W. S. Fenga, M. J. Jenga, D. W. Chene, K. L. Lee, "Cu2O-HTM/SiO2-ETM assisted for synthesis engineering improving efficiency and stability with heterojunction planar perovskite thin-film solar cells", Solar Energy, vol. 204, pp. 270-279. 2020.
[17] S. H. Hwang, J. Roh, J. Lee, J. Ryu, J. Yun, J. S. Jang, "Size-controlled SiO2 nanoparticles as scaffold layers in thin-film perovskite solar cells", Journal of Materials Chemistry A, vol. 2, no. 39, pp. 16429-16433. 2014.
[18] G. Niu, W. Li, F. Meng, L. Wang, H. Dong, Y. Qiu, "Study on the stability of CH3NH3PbI3 films and the effect of post-modification by aluminum oxide in all-solid-state hybrid solar cells", Journal of Materials Chemistry A, vol. 2, no. 3, pp. 705-710. 2014.
[19] X. Dong, X. Fang, M. Lv, B. Lin, S. Zhang, J. Ding, N. Yuan, "Improvement of the humidity stability of organic–inorganic perovskite solar cells using ultrathin Al2O3 layers prepared by atomic layer deposition", Journal of Materials Chemistry A, vol. 3, no. 10, pp. 5360-5367. 2015.
[20] D. Bi, S. J. Moon, L. Haggman, G. Boschloo, L. Yang, E. M. J. Johansson, M. K. Nazeeruddin, M. Gratzel, A. Hagfeldt, "Using a two-step deposition technique to prepare perovskite (CH3NH3PbI3) for thin film solar cells based on ZrO2 and TiO2 mesostructures", RSC Advances, vol. 3, no. 41, pp. 18762-18766. 2013.
[21] K. Mahmood, S. Sarwar M. T. Mehran, "Current status of electron transport layers in perovskite solar cells: materials and properties", RSC Advances, vol. 7, no. 28, 17044-17062. 2017.
[22] Q. Zhang, C. S. Dandeneau, X. Zhou, G. Cao, "ZnO Nanostructures for Dye-Sensitized Solar Cells", Advanced Materials, vol. 21, no. 41, pp. 4087-4108. 2009.

[23] Z. L. Wang, "Zinc oxide nanostructures: growth, properties and applications", Journal of Physics: Condensed Matter, vol. 16, no. 25, R829. 2004.
[24] H. Liu, Z. Huang, S. Wei, L. Zheng, L. Xiao, Q. Gong, "Nano-structured electron transporting materials for perovskite solar cells", Nanoscale, vol. 8, no. 12, pp. 6209-6221. 2016.
[25] C. C. Chueh, C. Z. Li, A. K. Y. Jen, "Recent progress and perspective in solution-processed Interfacial materials for efficient and stable polymer and organometal perovskite solar cells", Energy & Environmental Science, 8, no. 4. pp. 1160-1189. 2015.
[26] M. G. Ju, M. Chen, Y. Zhou, J. Dai, L. Ma, N. P. Padture, X. C. Zeng, "Toward Eco-friendly and Stable Perovskite Materials for Photovoltaics", Joule, vol. 2, pp. 1231-1241. 2018.
[27] M. Burgelman, K. Decock, S. Khelfi, A. Abass, "Advanced electrical Simulation of thin film solar cells", Thin solid films, vol. 535, pp. 296-309. 2013.
[28] A. Niemegeers, S. Gillis, M. Burgleman, "A user program for realistic simulation of polycrystalline heterojunction solar cells; SCAPS-1D", Proceedings of the 2nd world conference on photovoltaic energy conversion, Wein, 1998.
[29] M. Burgelman, K. Decock, A. Niemegeers, J. Verschruegen, S. Degrave, SCAPS Manual, 2016.
[30] L. Lin, L. Jiang, Y. Qiu, Y. Yu, "Modeling and analysis of HTM-free perovskite solar cells based on ZnO electron transport layer", Superlattices and Microstructures, 104, 167-177. 2017.
[31] O. A. Muhammed, E. Danladi, P. H. Boduku, J. Tasiu, M. S. Ahmad, N. Usman "Modelling and Simulation of lead-free perovskite solar cell using SCAPS-1D", East European Journal of Physics vol. 2021, no. 2, pp. 146-154. 2021.
[32] H. J. Du, W. C. Wang, J. Z. Zhu, "Device simulation of lead-free CH3NH3SnI3 perovskite solar cells with high efficiency", Chinese Physics B, vol. 25, no. 10, 108801. 2016.
[33] R. Wei, "Modelling of Perovskite Solar Cells", M.Sc. thesis, Queensland University of Technology, 2018.
[34] S. Aseena, A. Nelsa, V. S. Babu, "Optimization of layer thickness of ZnO based perovskite solar cells using SCAPS 1D", Materials Today: Proceedings, vol. 43, 3432-3437. 2020.
[35] D. Jalalian, A. Ghadimi, A. Kiani, "Modeling of a high performance bandgap graded Pb-free HTM-free perovskite solar cell", The European Physical Journal Applied Physics, vol. 87, 10101. 2019.
[36] K. Nishimura, M. A. Kamarudin, D. Hirotani, K. Hamad, Q. Shen, S. Iikubo, T. Minemoto, K. Yoshino, S. Hayase, "Lead-free tin-halide perovskite solar cells with 13% efficiency", Nano Energy, vol. 74, 104858. 2020.
[37] C. Momblona, O. Malinkiewicz, C. Roldan-Carmona, A. Soriano, L. Gil-Escrig, E. Bandiello, M. Scheepers, E. Edri, H. J. Bolink, "Efficient methylammonium lead iodide perovskite solar cells with active layers from 300 to 900 nm", Applied Materials, vol. 2, 081504. 2014.
[38] S. Rai, B. K. Pandey, D. K. Dwivedi, "Designing hole conductor free tin–lead halide based all-perovskite heterojunction solar cell by numerical simulation", Journal of Physics and Chemistry of Solids, vol. 156, 110168. 2021.
[39] K. R. Adhikari, S. Gurung, B. K. Bhattarai, B. M. Soucase, "Comparative study on MAPbI3 based solar cells using different electron transporting materials", Physica Status Solidi C, vol. 13, no. 1, pp. 13-17. 2016.
[40] F. Hao, C. C. Stoumpos, C. D. Hanh, R. P. H. Chang, M. G. Kanatzidis, "Lead-free solid-state organic–inorganic halide perovskite solar cells", Nature Photonics, vol. 8, no. 6, pp. 489-494. 2014.
[41] L. Huang, X. Sun, C. Li, R. Xu, J. Xu, Y. Du, Y. Wu, J. Ni, H. Cai, J. Li, Z. Hu, J. Zhang, "Electron transport layer-free planar perovskite solar cells: Further performance enhancement perspective from device simulation", Solar Energy Materials & Solar Cells, vol. 157, pp. 1038-1047. 2016.
[42] W. Ke, G. Fang, J. Wan, H. Tao, Q. Liu, L. Xiong, P. Qin, J. Wang, H. Lei, G. Yang, M. Qin, X. Zhao, Y. Yan, "Efficient hole-blocking layer-free planar halide perovskite thin-film solar cells", Nature Communications, vol. 6, 6700. 2015.
[43] N. F. Mott, E. A. Davis, "Electronic Processes in Non-Crystalline Materials" 2nd edition Clarendon, Oxford, 1979.